APPENDIX DR1: GEOCHRONOLOGY OF MAGMATISM

BOYONGAN AND BAYUGO INTRUSIVE GEOCHRONOLOGY

Copper-gold mineralization at Boyongan and Bayugo occurred during multiphase intrusive activity. The basis of the U-Pb dating method applied herein is the decay of ^{238}U through a series of radioactive daughter isotopes to produce stable ^{206}Pb and ^{4}He, with an equilibrium half-life of 4.468 Ga (Faure, 1986). The degree of weathering and hydrothermal alteration that has affected the intrusions at Boyongan and Bayugo emphasizes the need for a robust geochronometer to constrain the crystallization history. Zircon is a common accessory mineral in intermediate and felsic igneous rocks and commonly contains 10^2-10^3 ppm U, making it a viable mineral for U-Pb age determinations. In addition, the closure temperature for Pb retention in zircon is high, exceeding 900˚C (Lee et al., 1997). With a closure temperature in the range of the crystallization temperature of intermediate magmas, U-Pb age determinations of zircon can provide close approximations of the crystallization age for the intrusions, and are less subject to partial or complete resetting due to thermal perturbations than other geochronometers (e.g. Ar-Ar biotite, Harrison and Zeitler, 2005).

METHODOLOGY

Material to constrain the absolute timing and duration of magmatism focused on a suite of four samples representing the earliest and latest intrusive phases in the complex (Figure DR1). The sampling targeted intrusive phases from least-altered, unweathered, and coherent portions of the intrusive complex, and ranged between 2.5 and 5.0 kg each. Two samples from the early diorite complex (BEP and MGD) were selected to represent the earliest recognized intrusive events. Samples from the late-mineralization diorite porphyry phases at Boyongan (LDP) and Bayugo (DIO4) represent the youngest recognized intrusive events in these areas.

Zircon separations were performed at the University of Tasmania. After each sample was crushed and sieved to <0.425 mm, a combination of panning and heavy liquid separation provided heavy mineral concentrates. From these between 19 and 24 zircon grains from each sample were selected for dating. Zircon grains selected were generally euhedral-subhedral, doubly-terminated crystals, ranging in length between 50 μm and 25 μm (Figures DR2-DR3).

At the Australian National University (ANU) Research School of Earth Sciences the grains were mounted in polished epoxy disks, along with chips of reference zircons FC1 and SL13. Once polished, cathodo-luminescence (CL) imaging of the zircon grains highlighted characteristics of their growth history to enable better targeting with the ion microprobe. The CL imaging revealed simple growth zoning with no evidence of inherited cores (Figures DR2-DR3). The zircon grains were analyzed at ANU using the Sensitive High-Resolution Ion Microprobe (SHRIMP)-2 method for U-Pb, with between 18 and 22 spot analyses per sample (not including reference zircons). Spot analyses generally focused on zircon rims, targeting the youngest stages of zircon growth banding as highlighted by the CL imaging. The analyses consisted of six scans of the mass range for samples and the reference zircons.

The data were reduced in a manner similar to that described by in Williams (1998, and references therein). Ages were calculated using common Pb-corrected $^{238}U/^{206}Pb$ ratios, with common lead determined using measured $^{207}Pb/^{206}Pb$ and $^{238}U/^{206}Pb$ ratios after the methodology of Tera and Wasserburg (1972), and Williams (1998). The Pb/U ratios were normalized relative to a value of 0.1859 for the $^{206}Pb/^{238}U$ ratio of the FC1 reference zircon, equivalent to an age of 1099 Ma (Paces and Miller, 1993). Ages were calculated as weighted means with uncertainties based on the errors associated with the sample analyses. The precision on the FC1 analyses obtained in the same analytical sessions as the samples was 0.2%, and so contributes a negligible error to the reported ages.

RESULTS OF U-Pb SHRIMP-2 ZIRCON AGE DETERMINATIONS

Table DR1 summarizes the data for each SHRIMP spot analysis. With one exception at 92.7 Ma, dates for the 78 individual analyses ranged between 1.0 and 2.9 Ma. In this age range, these results represent approximately 0.04% of the ^{238}U-^{206}Pb half life of 4.5 Ga. Because the radiogenic ^{206}Pb component is small in young zircons, common ^{206}Pb can represent a large proportion of the total ^{206}Pb in such samples, a problem compounded by low-U zircons. Calculation of $^{238}U/^{206}Pb$ ages therefore excluded nine spot analyses with a high proportion (> 39%) of common ^{206}Pb, because these samples inflated the uncertainty in the common-Pb-corrected age determinations (italicized records in table DR1) . Figures DR2 and DR3 present the CL images, error-weighted age spectra, and Tera-Wasserburg concordia plots for each sample.

Common Pb-corrected mean age determinations for the four samples ranged between 2.3 and 2.1 Ma (Table DR2). At the 2σ level, all four results are indistinguishable within analytical uncertainty. However, mean ages for the pre-mineralization early diorite complex (2.3 ± 0.1 and 2.2 ± 0.1 Ma) are both older than that of the youngest identified intrusion (2.3 ± 0.2 Ma), consistent with relative ages based on cross-cutting relationships. Figure DR4 presents these analytical results within the context of relative age for the intrusions, as determined by field relationships.

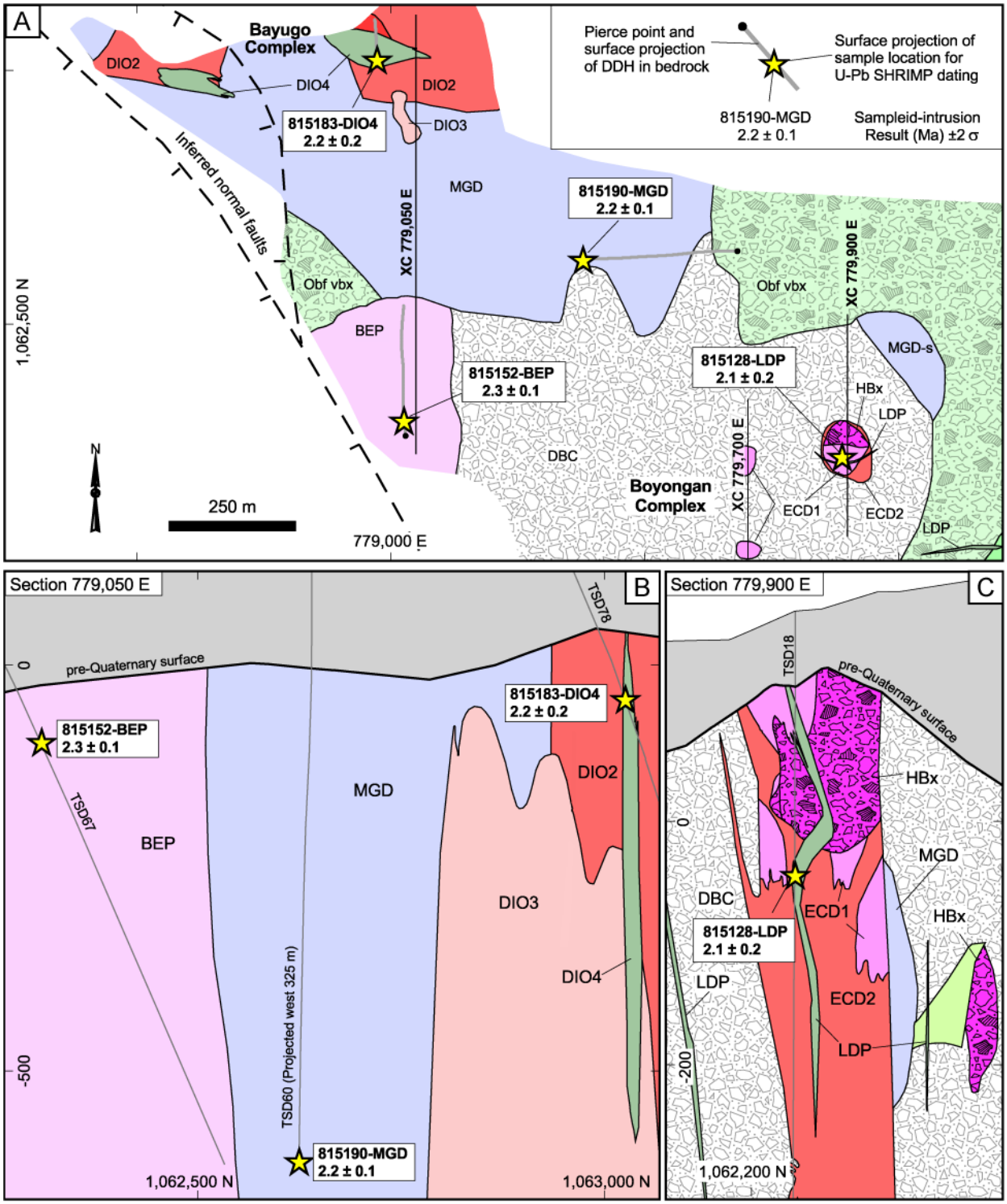

Figure DR1. Sampling locations, geological context, and results of U-Pb SHRIMP zircon dating of intrusions at Boyongan and Bayugo. **A**: Plan view showing the sample locations projected to the pre-Quaternary paleosurface. **B**: Cross-section along 779,050E showing sample locations for intrusions of the early diorite complex (BEP and MGD), and for the late-mineralization diorite porphyry (DIO4) at Bayugo. **C**: Cross-section along 779,900E through the eastern high-grade zone showing sample location for the late-mineralization diorite porphyry (LDP) at Boyongan. Cross-section locations for (B) and (C) given in (A). The legend at the end of the Appendix provides a detailed explanation of rock types.

Table DR1. Summary of SHRIMP U-Pb zircon spot analyses

Grain & spot	U (ppm)	Th (ppm)	Th/U	$^{204}Pb/^{206}Pb$	f_{206} (%)[1]	Total $^{238}U/^{206}Pb$	Unc.[2]	Total $^{207}Pb/^{206}Pb$	Unc.[2]	Radiogenic $^{206}Pb/^{238}U$	Unc.[2]	Age (Ma)[3]	Unc.[2] (Ma)
815152 Early diorite complex: bird's-eye diorite porphyry (BEP)													
1.1	436	114	0.26	0.012068	11.02	2463	80	0.1331	0.0130	0.00036	0.00001	2.33	0.09
2.1	435	120	0.28	0.016120	4.46	2772	95	0.0813	0.0107	0.00034	0.00001	2.22	0.08
3.1	262	49	0.19	0.019599	9.12	2636	111	0.1181	0.0163	0.00034	0.00002	2.22	0.11
4.1	394	109	0.28	-	0.30	2724	96	0.0485	0.0105	0.00037	0.00001	2.36	0.09
5.1	218	51	0.24	0.052916	10.35	2380	101	0.1278	0.0169	0.00038	0.00002	2.43	0.12
6.1	309	59	0.19	0.010045	9.31	2650	106	0.1196	0.0169	0.00034	0.00002	2.21	0.11
7.1	359	100	0.28	-	5.68	2547	127	0.0910	0.0130	0.00037	0.00002	2.39	0.13
8.1	323	54	0.17	0.012746	3.63	2604	129	0.0747	0.0110	0.00037	0.00002	2.39	0.12
9.1	189	39	0.21	0.040335	37.72	1767	79	0.3439	0.0670	0.00035	0.00006	2.27	0.37
10.1	528	225	0.43	0.013111	5.63	2753	83	0.0905	0.0096	0.00034	0.00001	2.21	0.07
10.2	*413*	*122*	*0.29*	*0.015020*	*7.29*	*2357*	*76*	*0.1036*	*0.0113*	*0.00039*	*0.00001*	*2.54*	*0.09*
10.3	325	106	0.33	0.004575	8.15	2689	101	0.1105	0.0148	0.00034	0.00002	**2.20**	**0.10**
11.1	*28*	*2*	*0.07*	*0.106236*	*42.59*	*2093*	*358*	*0.3824*	*0.1341*	*0.00027*	*0.00010*	*1.77*	*0.63*
12.1	240	40	0.17	0.004706	3.14	2686	121	0.0709	0.0152	0.00036	0.00002	2.32	0.12
13.1	595	513	0.86	-	1.57	2612	83	0.0585	0.0089	0.00038	0.00001	2.43	0.08
13.2	246	51	0.21	0.026114	5.87	2576	111	0.0925	0.0148	0.00037	0.00002	2.36	0.11
14.1	458	172	0.38	0.017170	6.30	2590	80	0.0958	0.0103	0.00036	0.00001	2.33	0.08
15.1	226	45	0.20	-	12.40	2397	103	0.1440	0.0185	0.00037	0.00002	2.36	0.13
815090 Early diorite complex: medium-grained diorite porphyry (MGD)													
1.1	374	206	0.55	0.024025	0.61	2779	111	0.0509	0.0126	0.00036	0.00002	2.31	0.10
2.1	270	149	0.55	0.025898	15.47	2406	104	0.1682	0.0207	0.00035	0.00002	2.26	0.13
3.1	147	66	0.45	-	4.97	2639	203	0.0854	0.0252	0.00036	0.00003	2.32	0.20
4.1	204	78	0.38	0.022554	21.01	2183	104	0.2120	0.0288	0.00036	0.00003	2.33	0.17
5.1	273	102	0.37	0.024847	7.10	2938	129	0.1021	0.0157	0.00032	0.00002	2.04	0.10
6.1	470	412	0.88	0.004129	14.58	2334	73	0.1612	0.0167	0.00037	0.00002	2.36	0.11
7.1	156	53	0.34	0.012124	11.43	2753	255	0.1364	0.0305	0.00032	0.00003	2.07	0.21
8.1	261	113	0.43	0.001697	6.98	2952	205	0.1012	0.0203	0.00032	0.00002	**2.03**	**0.15**
9.1	245	114	0.47	0.029598	19.07	2336	97	0.1967	0.0610	0.00035	0.00004	2.23	0.24
10.1	375	267	0.71	0.028986	15.53	2386	94	0.1687	0.0196	0.00035	0.00002	2.28	0.12
11.1	149	59	0.39	-	7.73	2508	140	0.1071	0.0243	0.00037	0.00002	2.37	0.16
12.1	264	117	0.44	0.037456	39.96	1733	66	0.3617	0.0263	0.00035	0.00004	2.23	0.24
13.1	348	216	0.62	0.013799	2.20	2721	107	0.0635	0.0124	0.00036	0.00002	2.32	0.10
14.1	260	123	0.47	-	4.08	2787	128	0.0783	0.0171	0.00034	0.00002	2.22	0.11
15.1	331	194	0.59	0.004701	2.79	2720	108	0.0681	0.0136	0.00036	0.00002	2.30	0.10
16.1	278	149	0.54	0.029317	6.79	2649	110	0.0997	0.0147	0.00035	0.00002	2.27	0.11
17.1	325	121	0.37	0.005309	30.30	2041	208	0.2854	0.0221	0.00034	0.00004	2.20	0.27
18.1	*85*	*23*	*0.27*	*0.084682*	*39.82*	*2521*	*187*	*0.3605*	*0.0566*	*0.00024*	*0.00004*	*1.54*	*0.25*
19.1	109	32	0.30	0.020323	38.18	1822	109	0.3476	0.0465	0.00034	0.00005	2.19	0.30
20.1	222	77	0.35	0.013825	6.08	2929	242	0.0941	0.0201	0.00032	0.00003	2.07	0.18
21.1	450	214	0.48	-	4.15	2977	109	0.0789	0.0126	0.00032	0.00001	2.08	0.08
22.1	547	569	1.04	0.012519	4.47	2695	86	0.0814	0.0100	0.00035	0.00001	2.28	0.08

Table DR1 (Continued)

Grain & spot	U (ppm)	Th (ppm)	Th/U	$^{204}Pb/^{206}Pb$	f_{206} (%)[1]	Total $^{238}U/^{206}Pb$	Unc.[2]	Total $^{207}Pb/^{206}Pb$	Unc.[2]	Radiogenic $^{206}Pb/^{238}U$	Unc.[2]	Age (Ma)[3]	Unc.[2] (Ma)
815183 Bayugo: late-mineralization diorite porphyry (DIO4)													
1.1	*97*	*45*	*0.46*	*0.079736*	*87.66*	*633*	*84*	*0.7383*	*0.0403*	*0.00019*	*0.00019*	*1.26*	*1.25*
2.1	*86*	*36*	*0.42*	*0.050587*	*59.29*	*1041*	*51*	*0.5143*	*0.0505*	*0.00039*	*0.00010*	*2.52*	*0.62*
3.1	*60*	*22*	*0.36*	*0.001875*	*0.70*	*69*	*2*	*0.0534*	*0.0041*	*0.01448*	*0.00051*	*92.70*	*3.22*
4.1	321	441	1.37	0.001118	20.78	2138	77	0.2102	0.0190	0.00037	0.00002	2.39	0.14
6.1	115	37	0.32	0.010294	5.99	2722	182	0.0934	0.0333	0.00035	0.00003	2.23	0.18
7.1	184	54	0.30	0.017516	7.24	2621	134	0.1032	0.0184	0.00035	0.00002	2.28	0.13
8.1	271	227	0.84	0.053563	9.33	2549	110	0.1197	0.0164	0.00036	0.00002	2.29	0.12
9.1	127	43	0.33	0.025314	8.15	2698	166	0.1105	0.0239	0.00034	0.00002	2.19	0.15
10.1	*101*	*39*	*0.39*	*0.044285*	*88.35*	*792*	*32*	*0.7437*	*0.0475*	*0.00015*	*0.00016*	*0.95*	*1.03*
11.1	321	163	0.51	0.021507	5.88	2747	112	0.0925	0.0173	0.00034	0.00002	2.21	0.10
12.1	151	76	0.50	0.051496	13.07	2593	184	0.1493	0.0232	0.00034	0.00003	2.16	0.17
13.1	209	108	0.52	0.042560	16.14	2563	123	0.1735	0.0227	0.00033	0.00002	2.11	0.13
14.1	*127*	*67*	*0.53*	*0.048406*	*80.62*	*436*	*131*	*0.6828*	*0.0510*	*0.00044*	*0.00031*	*2.87*	*1.98*
15.1	128	45	0.35	0.032780	38.20	1879	97	0.3477	0.0386	0.00033	0.00004	2.12	0.26
16.1	97	27	0.27	0.013640	9.01	2816	214	0.1172	0.0376	0.00032	0.00003	2.08	0.19
17.1	136	45	0.33	-	5.27	3006	267	0.0877	0.0321	0.00032	0.00003	2.03	0.20
18.1	220	135	0.61	-	0.09	3059	167	0.0468	0.0181	0.00033	0.00002	2.11	0.12
19.1	148	80	0.54	0.064940	18.55	2610	199	0.1926	0.0304	0.00031	0.00003	**2.01**	**0.19**
815128 Boyongan: late-mineralization diorite porphyry (LDP)													
1.1	118	46	0.39	0.015783	27.36	1971	106	0.2622	0.0332	0.00037	0.00003	2.38	0.22
2.1	157	167	1.07	0.037459	33.69	1863	85	0.3122	0.0310	0.00036	0.00004	2.29	0.23
3.1	108	46	0.43	-	7.87	2734	191	0.1082	0.0372	0.00034	0.00003	2.17	0.19
4.1	210	163	0.77	0.021971	13.29	2868	145	0.1510	0.0224	0.00030	0.00002	1.95	0.12
5.1	*57*	*19*	*0.34*	*0.042752*	*87.39*	*367*	*23*	*0.7362*	*0.0454*	*0.00034*	*0.00034*	*2.21*	*2.19*
6.1	75	28	0.37	0.075330	16.59	2729	387	0.1771	0.0457	0.00031	0.00005	1.97	0.31
7.1	*100*	*35*	*0.35*	*0.015114*	*67.16*	*1027*	*198*	*0.5765*	*0.1927*	*0.00032*	*0.00026*	*2.06*	*1.67*
8.1	73	28	0.38	0.008711	10.90	2811	243	0.1321	0.0404	0.00032	0.00003	2.04	0.21
9.1	78	21	0.27	0.128922	31.88	2138	154	0.2978	0.0512	0.00032	0.00004	2.05	0.27
10.1	*27*	*8*	*0.31*	*0.179911*	*48.31*	*2195*	*244*	*0.4275*	*0.0990*	*0.00024*	*0.00007*	*1.52*	*0.44*
11.1	82	31	0.37	-	5.62	2618	195	0.0905	0.0376	0.00036	0.00003	2.32	0.21
12.1	92	33	0.36	0.035042	-0.53	2607	179	0.0419	0.0267	0.00039	0.00003	2.49	0.19
13.1	141	43	0.30	0.012678	13.71	2547	135	0.1544	0.0260	0.00034	0.00002	2.18	0.15
14.1	78	25	0.33	0.027487	17.84	2804	210	0.1869	0.0412	0.00029	0.00003	1.89	0.19
15.1	69	24	0.34	0.089921	10.12	2833	228	0.1260	0.0280	0.00032	0.00003	2.04	0.19
16.1	133	51	0.39	-	-0.56	2498	141	0.0417	0.0197	0.00040	0.00002	2.59	0.16
17.1	49	16	0.32	-	4.16	2837	305	0.0790	0.0897	0.00034	0.00005	2.18	0.35
18.1	74	43	0.59	-	36.68	1829	116	0.3358	0.0491	0.00035	0.00005	2.23	0.31
19.1	128	37	0.29	-	9.34	3219	219	0.1198	0.0410	0.00028	0.00003	**1.82**	**0.16**
20.1	80	21	0.27	0.048210	14.05	2701	199	0.1570	0.0375	0.00032	0.00003	2.05	0.19

[1] f_{206} % denotes the percentage of ^{206}Pb that is common Pb. Correction for common Pb made using the measured $^{238}U/^{206}Pb$ and $^{207}Pb/^{206}Pb$ ratios following Tera and Wasserburg (1972) as outlined in Williams (1998).

[2] Uncertainties (Unc.) given at the one σ level.

[3] Age determination based on $^{206}Pb/^{238}U$ system.

Analyses in italics were excluded from the calculation of the mean sample age (see Appendix text for discussion). Results in bold represent the youngest individual age determinations for each sample.

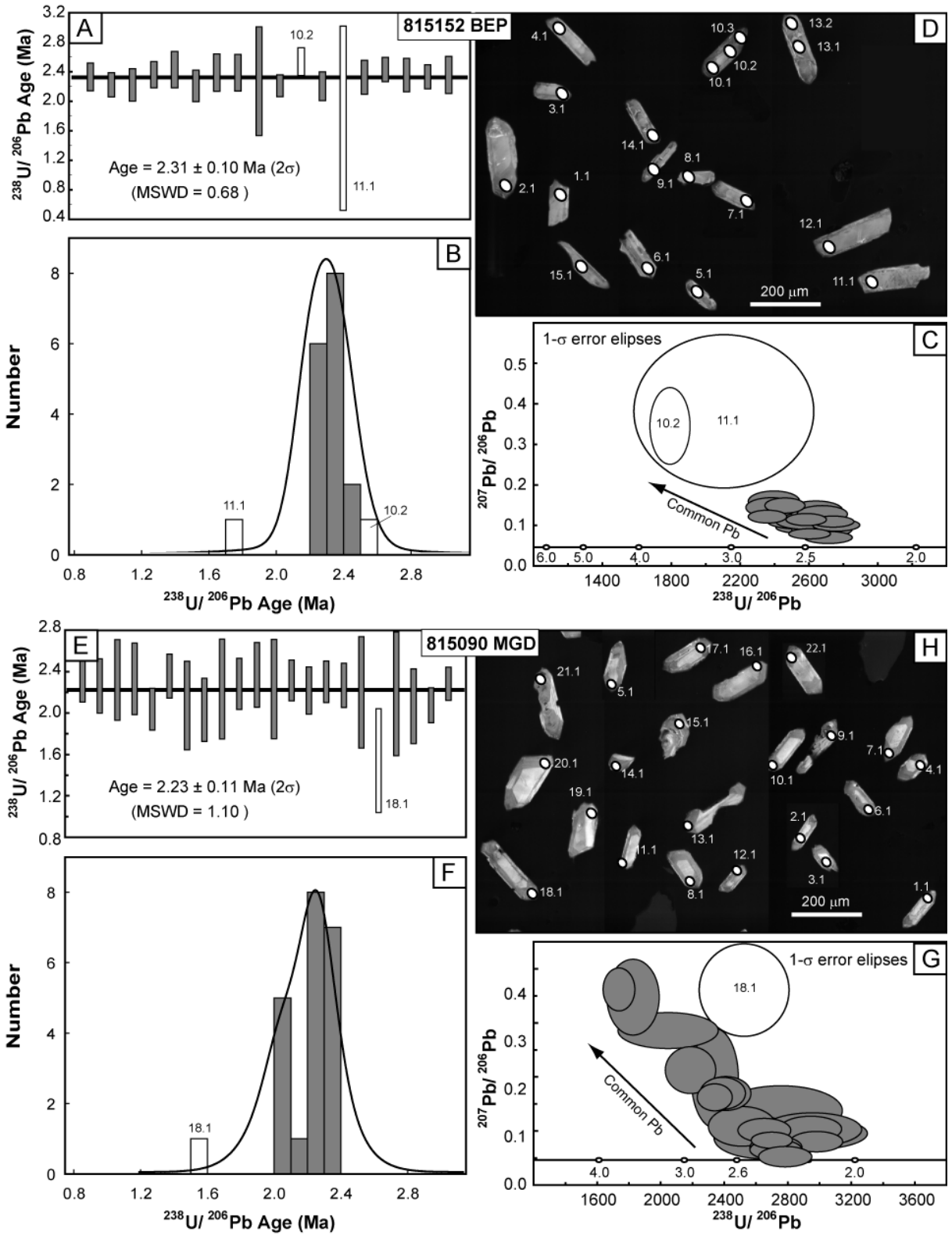

Figure DR2. Details of SHRIMP U-Pb zircon dating of samples from the early diorite complex. Filled gray symbols (bars and ellipses) represent spot analyses used in the age calculation for each sample. White bars and ellipses (labeled by grain and spot analysis; Table DR1) represent spot analyses excluded from the sample age calculation. A-D: sample 815152, bird's-eye diorite porphyry (BEP). **A**: Age and uncertainty (2-σ) for each spot analysis. Analysis 10.2 was excluded from the age calculation because it was made in a measurably older zircon core (D). **B**: Histogram for the spot analyses retained for the sample age calculation showing a normal distribution. **C**: Tera-Wasserburg plot showing common ^{206}Pb divergence from the $^{207}Pb/^{206}Pb$-$^{238}U/^{206}Pb$ concordia. **D**: Cathodo-luminescence images of zircon grains showing locations of spot analyses. E-H: sample 815096, medium-grained diorite porphyry (MGD). **E**: Age and uncertainty (2-σ) for each spot analysis. **F**: Histogram for the analyses retained for the sample age calculation. **G**: Tera-Wasserburg plot showing common ^{206}Pb divergence from the $^{207}Pb/^{206}Pb$-$^{238}U/^{206}Pb$ concordia. **H**: Cathodo-luminescence images of zircon grains showing locations of spot analyses.

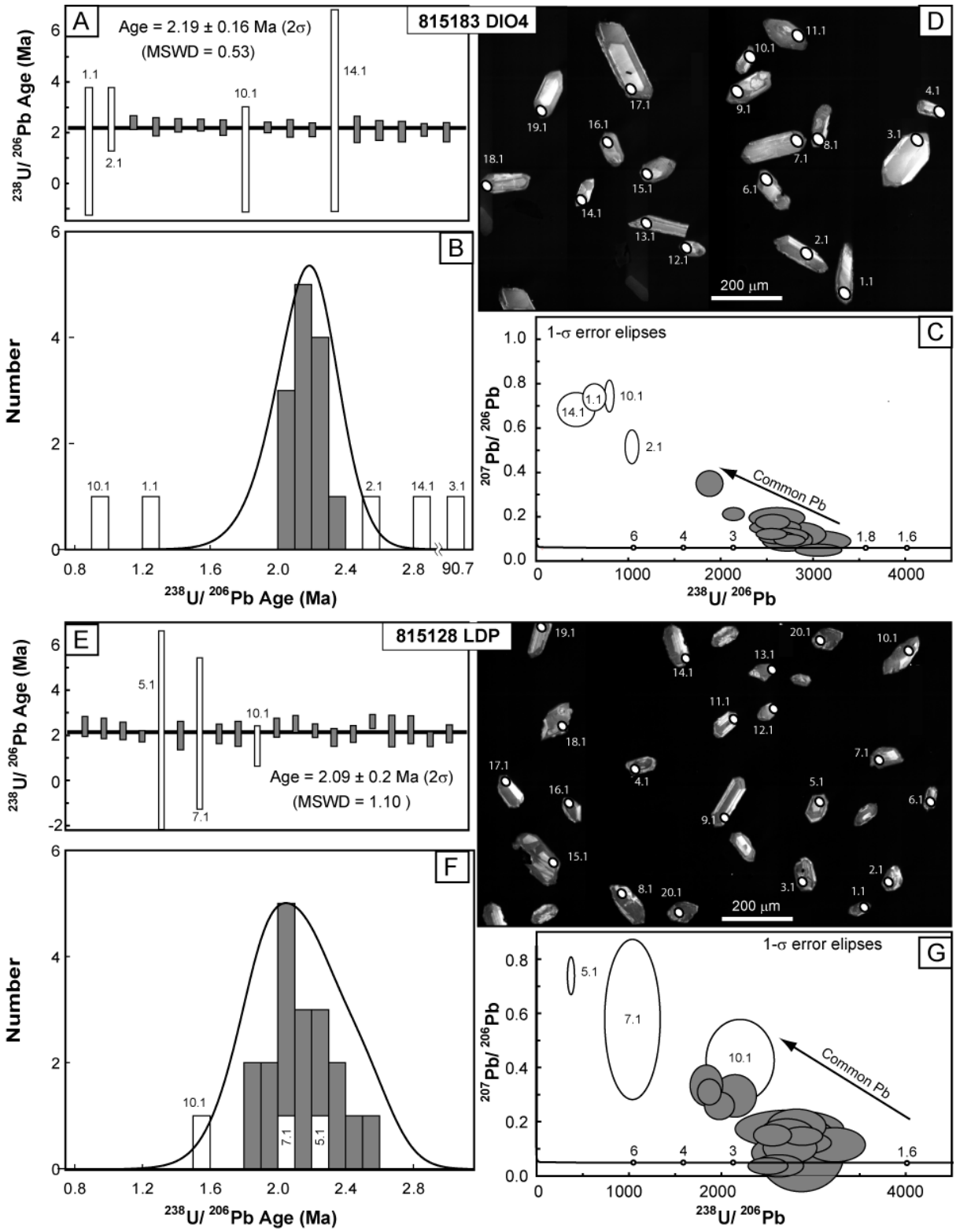

Figure DR3. Details of SHRIMP U-Pb zircon dating of samples from late-mineralization diorite porphyries. Filled gray symbols (bars and ellipses) represent spot analyses used in the age calculation for each sample. White bars and ellipses (labeled by grain and spot analysis; Table DR1) represent spot analyses excluded from the sample age calculation. A-D: sample 815183, Bayugo diorite porphyry DIO4. **A**: Age and uncertainty (2-σ) for each spot analysis. Analysis 3.1 (92.7 Ma) was excluded from the age calculation. **B**: Histogram for the spot analyses retained for the sample age calculation showing a normal distribution. **C**: Tera-Wasserburg plot showing common ^{206}Pb divergence from the ^{207}Pb/^{206}Pb-^{238}U/^{206}Pb concordia. **D**: Cathodo-luminescence images of zircon grains showing locations of spot analyses. E-H: sample 815128, Boyongan diorite porphyry LDP. **E**: Age and uncertainty (2-σ) for each spot analysis. **F**: Histogram for the analyses retained for the sample age calculation showing a normal distribution. **G**: Tera-Wasserburg plot showing common ^{206}Pb divergence from the ^{207}Pb/^{206}Pb-^{238}U/^{206}Pb concordia. **H**: Cathodo-luminescence images of zircon grains showing locations of spot analyses.

Table DR2. Sampling location and results for U-Pb SHRIMP II dating of igneous zircon

Sample	DDH and depth	Intrusion	Timing	Age (Ma)	Unc. (Ma)[/1]
815152	TSD67 392.2 m.	Bird's-eye diorite porphyry (BEP)	Early diorite stocks: predate diatreme breccia	2.3	0.1
815090	TSD60 948.6 m.	Medium-grained diorite porphyry (MGD)		2.2	0.1
815183	TSD78 451.32 m.	Late-mineralization diorite porphyry 4 (DIO4)	Youngest intrusive phase recognized at Bayugo	2.2	0.2
815128	TSD18 216.02 m.	Late-mineralization diorite porphyry (LDP)	Youngest intrusive phase recognized at Boyongan	2.1	0.2

[/1] Uncertainty (Unc.) reported at 2σ level.

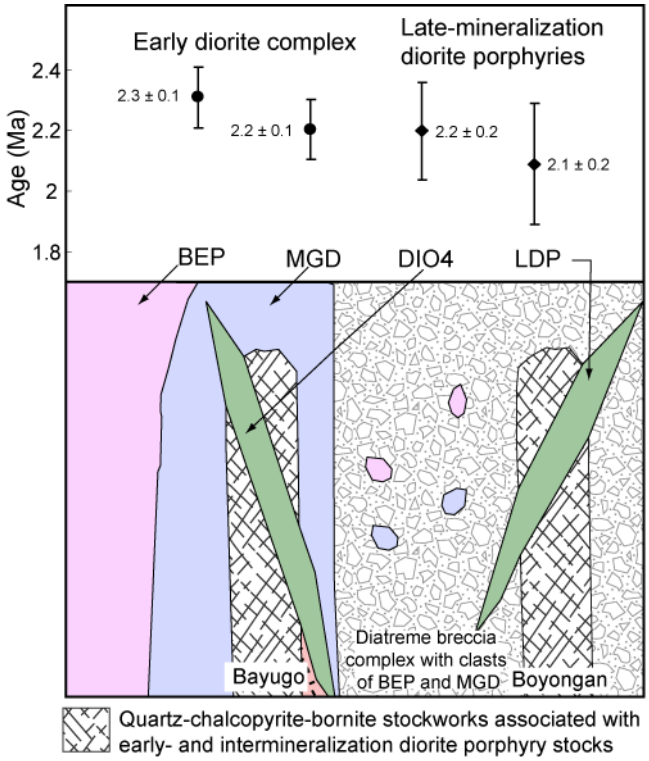

Figure DR4. SHRIMP U-Pb zircon age determinations and schematic diagram depicting relative and absolute age constraints for the intrusions dated. Intrusions dated from the early diorite complex (BEP and MGD) also occur as clasts within the diatreme breccia complex. Early- and intermineralization diorite stocks intruded the breccia complex, in association with and copper and gold mineralization in quartz vein stockworks. Late-mineralization diorite porphyry dikes (LDP and DIO4) truncated the mineralized intrusions. Although the age determinations are within analytical uncertainty (at 2σ), mean ages young in a manner consistent with field constraints for relative age. Mean ages for the earliest phases of magmatism (BEP and MGD) exceed 2.2 Ma, while those for the final intrusive phases (DIO4 at Bayugo and LDP at Boyongan) are younger than 2.2 Ma.

APPENDIX DR2: HYDROTHERMAL GEOCHRONOLOGY

INTRODUCTION

Paragenetic relationships demonstrate that illite-pyrite alteration followed K-silicate alteration at Boyongan and Bayugo. Age determinations of late K-silicate-stage molybdenite and of illite from post-K-silicate-alteration stages are used to constrain the absolute timing of the waning stages of hydrothermal activity.

TIMING OF PORPHYRY VEINING: RE-OS DATING OF MOLYBDENITE

Molybdenite selected for the Re-Os age determination (sample 819306) came from a stage-3b quartz vein (Braxton, 2007) associated with the intermineral diorite porphyry (IMD) at Boyongan (**Figure DR5A**). This is the youngest of the quartz veining events associated with the IMD magmatic-hydrothermal cycle (Figure 5.21 in Braxton, 2007). It is also the last K-silicate quartz vein stage of volumetric significance at Boyongan, as quartz veins in the later LDP dikes are not abundant.

Age determinations of hydrothermal molybdenite are based on the Re-Os method, whereby ^{187}Re decays to stable ^{187}Os with a half life of 41.6 Ga (Smoliar et al., 1996). Coarse-grained molybdenite was separated from a sample of vein quartz and prepared for dating at Colorado State University AIRIE center. The anticipated young age (relative to the Re-Os half-life) prompted the use of the double-Os-spike method (Markey et al., 2003). **Table DR3** presents the results of the Re-Os dating for two mineral separates from sample 819306. The replicate age determinations of 2.120 ± 0.007 and 2.115 ± 0.008 Ma are in close agreement. Despite the young age, extremely high Re concentrations (>2000 ppm) contributed to small analytical uncertainties. These results represent the youngest Re-Os molybdenite age determination yet reported.

TIMING OF ILLITE ALTERATION: K-AR DATING

Two samples of illite were selected for K-Ar age determinations. Sample 819574 came from a zone of intense illite-pyrite alteration (Braxton, 2007, Section 5.4.5.3) that had overprinted the K-silicate-stage quartz-vein stockwork in the eastern high-grade zone at Boyongan (**Figure DR5A**). Sample 814778 came from a debris flow in the Tugunan Formation covering the southern flank of the Boyongan deposit (**Figure DR5B**). These debris flows contain intensely illite-pyrite-altered diorite porphyry clasts in an illite-rich matrix (Braxton, 2007, Sections 3.3.7.1 and 5.4.5.3) and are thought to have been derived from erosion of a shallow clay-rich lithocap related to the hydrothermal system at Boyongan and Bayugo. Age determinations on hydrothermal illite were based on the K-Ar method, for which unstable ^{40}K decays by a branched scheme to stable ^{40}Ar and ^{40}Ca, with a total half life of 1.2505 Ga (Steiger and Jager, 1977).

Clay-sized (<2 μm) separates of illite were prepared at the University of Utah as follows:

1) Vein-quartz-free regions of the clay-rich samples were collected by excision with a diamond saw. Rock samples were then crushed lightly with a large ceramic mortar and pestle to approximately < 4 mm.

2) Aliquots of 20-40 g of crushed material were mixed with 200 ml of a 0.05% Calgon peptizing solution, and dispersed by blending for two minutes in glass Oesterizer blender beaker. The dispersion was decanted evenly into four 100-ml Nalgene® centrifuge tubes, each containing 50 ml.

3) The clays were further dispersed by placing the centrifuge tubes on a Beuhler ultramet III ultrasonic bath for 3 minutes.

4) After balance pairing, the coarse fraction was settled by centrifugation in a Sorval GLC-1 centrifuge at 500 rpm for 4.5 minutes using a HL-4 head.

5) The supernatant was decanted into four balance-paired 50 mL centrifuge tubes, and the 2-0.001 μm fraction settled in a Beckman G5-6 centrifuge at 6000 rpm for 6.0 minutes using a GA-10 head.

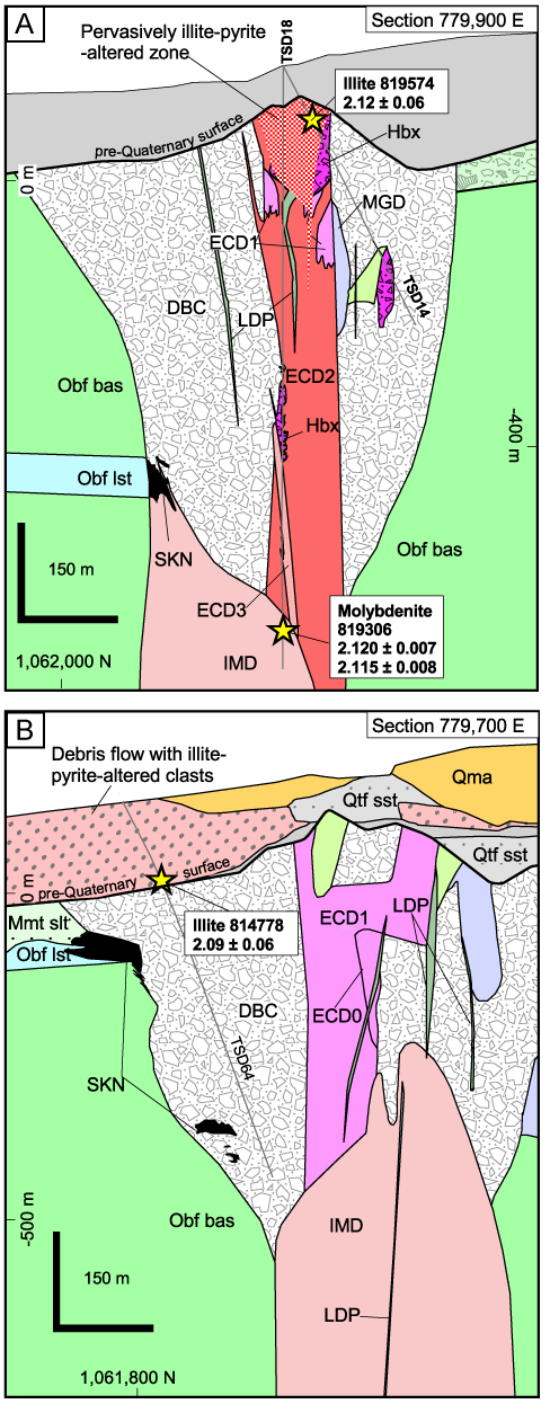

Figure DR5. Cross-sections along 779,900 E (A) and 779,700 E (B) depicting sample location, geological context, and results of dating of illite (K-Ar) and molybdenite (Re-Os) at Boyongan. Refer to **Figure DR1** for section locations. The legend at the end of the Appendices provides a detailed explanation of rock types.

6) If the supernatant following step 4 had little suspended material, the settled fraction in step 4 was re-dispersed in 200 ml of a 0.05% Calgon peptizing solution, and steps 3-5 repeated to maximize the amount of clay-sized material recovered.

7) After centrifugation in step 5, the supernatant was discarded and the <2 μm fraction oven-dried (60˚ C for 90 minutes) and the dry weight measured.

8) A thick slurry was made by mixing up to100 mg dried <2 μm material with de-ionized water at a ratio of approximately 1 ml (10-15 drops) water per 100 mg dried <2 μm material. The thick slurry was applied to a 6.25 cm^2 area of a glass slide a minimum of 16 mg/cm^2, and allowed to air-dry for 3-5 days, creating an oriented clay smear.

9) Air-dried samples were analyzed by XRD and then bathed in ethylene glycol vapors at 60˚ C for a minimum of eight hours. Ethylene glycol-solvated samples were analyzed by XRD within two hours of removal.

The oriented clay samples were analyzed by XRD with Cu Kα radiation on a Rigaku D Max 2200 V X-ray diffractometer using a graphite crystal monochromater. Divergence and Soller slit settings were 1°, and the scattering slit was set to 0.1°. Scanning a range of 2-30° 2 θ, at 1° 2 θ / minute produced diffraction patterns with high intensity peaks, and minimal background noise. Clay minerals were identified by a rational series of diagnostic peak positions. Following XRD analysis, the spectral signature of each clay mineral separate was measured in the visible near-infrared and short-wavelength infrared (VNIR-SWIR) spectrum (350-2500 nm) using an analytical spectral device (ASD) FSP350-2500P spectrometer. The software Spectral Geologist (Merry et al., 1999) was used to interpret these data.

Once purity was confirmed by XRD the separated were dated at the Australian National University (ANU) Research School of Earth Sciences. At ANU, total potassium was determined by flame photometry, while argon was extracted by fusion in an induction heater and characterized isotopically by standard mass-spectrometry techniques. **Table DR4** presents the results of the K-Ar dating.

Table DR3. Re-Os data for molybdenite from Boyongan

AIRIE Run #	Re (ppm)[/1]	^{187}Os (ppb)[/1]	Age (Ma)	Unc. (Ma)[/2]
MDID-549	2063 (2)	45.81 (3)	2.120	0.007
MDID-555	2558 (2)	56.67 (8)	2.115	0.008

MDID-555 is a second mineral separate in the same sample (819306.943).

Assumed initial $^{187}Os/^{188}Os$ for age calculation = 0.2 ± 0.1

Decay constant used for ^{187}Re is $1.666 \times 10^{-11} yr^{-1}$ (Smoliar et al. 1996)

Age corrected for Re blank = 5.94 ± 0.06 pg, total Os = 1.208 ± 0.007 pg, $^{187}Os/^{188}Os$ = 0.456 ± 0.006

Ages calculated using $^{187}Os = {}^{187}Re\ (e^{lt} - 1)$ include all analytical and ^{187}Re decay constant uncertainties

Carius tube dissolution with double Os spike method (Markey et al. 2003) on 50 mg (MDID-549) and 10 mg (MDID-555) separates

[/1] Absolute uncertainties (shown in brackets) are at 2-σ level for last digit indicated

[/2] Age uncertainties (Unc.) reported at the 2-σ level

Table DR4. Replicate potassium determinations for illite

Sample Designation	Weight analyzed (g)	K (wt %)
819574 Illite	0.03234	6.223 ± 0.15
	0.04436	6.154 ± 0.35
814778 Illite	0.03177	7.445 ± 0.66
	0.02997	7.247 ± 0.13
	0.01677	7.486 ± 0.24
	0.01568	7.335 ± 0.20

Table DR4. K-Ar age determinations for illite

Sample	Mineral	K (wt%)	Unc. (%)[/1]	^{40}Ar (mol/gram)	Unc. (%)[/1]	Age (Ma)	Unc. (Ma)[/1]	%*Ar[/2]
814778	illite	7.378	1.47	2.677×10^{-11}	0.5	2.09	0.06	48.9
819574	illite	6.189	0.9	2.282×10^{-11}	0.25	2.12	0.06	33.9

[/1] Uncertainty (Unc.) reported at 2σ level.

[/2] Percentage of radiogenic Ar.

APPENDIX DR3: LOW-TEMPERATURE GEOCHRONOLOGY

METHODS

Samples for apatite (U-Th)/He dating were collected from six locations within the intrusive complex at Boyongan and Bayugo (**Figure DR6**) over a vertical interval of 630 m. The sampling targeted the least-altered and least-weathered portions of inter- and late-mineralization diorite porphyries, which were considered the most likely to contain apatite crystals of adequate size. Heavy mineral separates were prepared at the University of Tasmania by crushing 0.5-3.0 kg of each sample to <0.425 mm, followed by a combination of panning and heavy liquid separation.

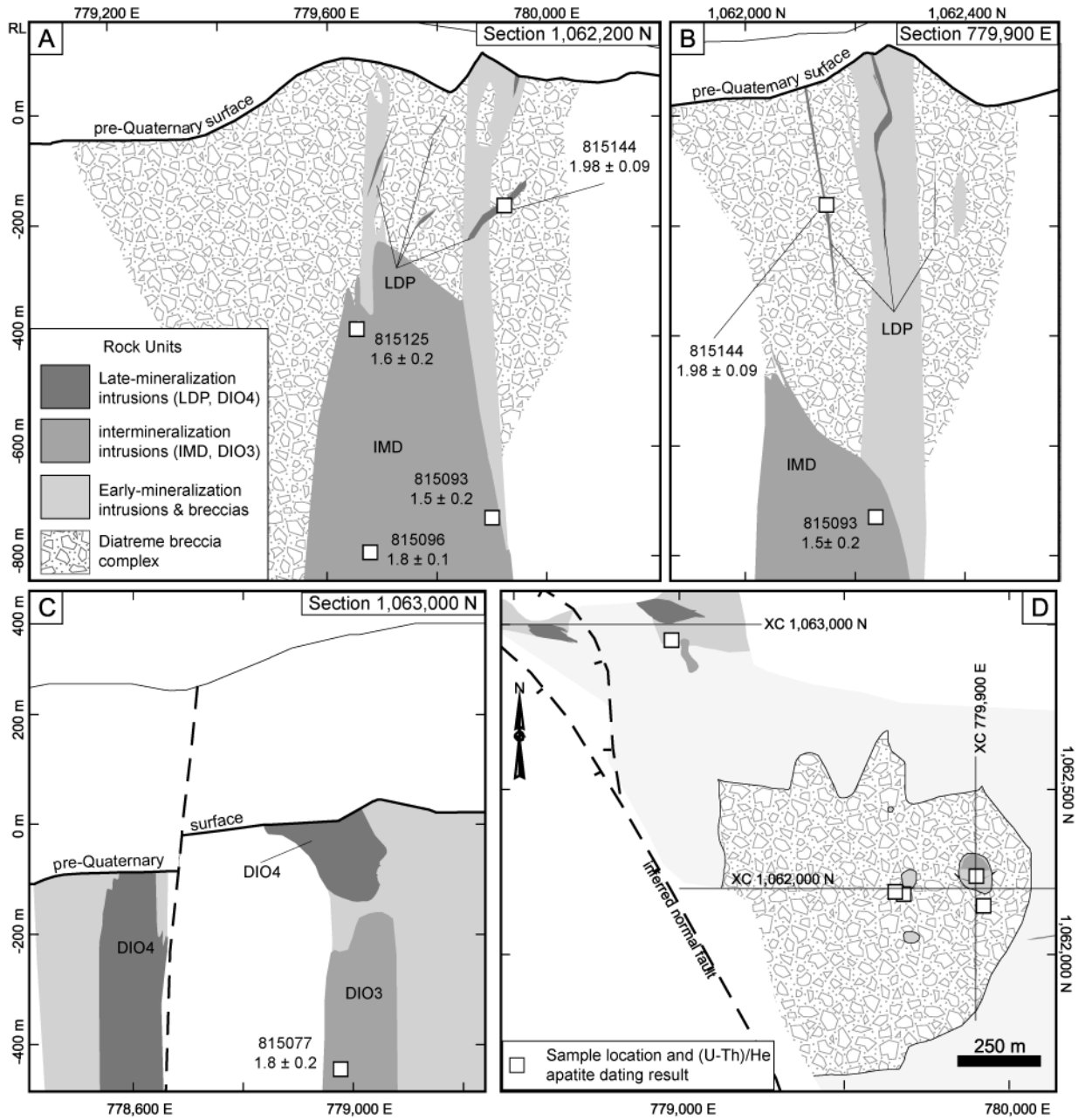

Figure DR6. Sample locations and results (in Ma) for (U-Th)/He dating of apatite from inter- and late-mineralization diorite porphyries (labelled) at Boyongan and Bayugo. Analytical uncertainty is reported at 2σ. **A**: Cross-section looking north along 1,062,200 N through the eastern and western high-grade zones at Boyongan. **B**: Cross-section looking west along 779,900 E through the eastern high-grade zone at Boyongan. **C**: Cross-section looking north along 1,063,000 N at Bayugo. **D**: Map view showing cross-section locations and lateral distribution of sample locations (projected to surface).

Apatite crystals were hand-selected at Yale University under a high-power (160x) binocular microscope using cross-polarized light to screen for inclusions. Apatites selected were the largest, most complete, and euhedral inclusion-free crystals in each separate. Helium was extracted by Nd:YAG laser-heating and analyzed on a quadruple mass-spectrometer. Following helium degassing, the apatite crystals were dissolved in HNO_3, and U, Th, and Sm determined on a Finnigan Element2 ICP-MS. Details of the selection, extraction, and analytical procedures are provided in Appendix B of Reiners et al. (Reiners et al., 2004).

RESULTS

Table DR5 presents the results of the apatite (U-Th)/He age determinations. Two results were from samples with the smallest apatite crystals, and yielded suspect or geologically unreasonable dates. One of these dates (7.5 Ma) was rejected because it was older than the source intrusive complex (2.3-2.1 Ma), as determined by U-Pb SHRIMP age determinations (**Appendix DR1**). A second result (0.5 Ma) was rejected in light of its small crystal radius (38 μm) and abraded character. The remaining five results range between 1.98 and 1.5 Ma (**Figure DR6**), with analytical uncertainties between 5% and 14% due to low U concentrations (2-3 ppm).

Table DR5. Apatite (U-Th)/He age determinations

Sample	RL (m)	Intrusion	ng U	ng Th	ng Sm	Raw age (Ma)	Corrected Age (Ma)	Unc. (Ma)[/1]	% Sm[/1]	Radius (μm)[/3]	Mass (μg)	U ppm	Th ppm	Th/U	^{4}He (nmol/g)	Crystal Morphology
815077	-447	DIO3	0.02	0.03	0.55	1.4	1.8	0.2	2.7	57	5.50	3.1	5.8	1.9	0.03	End chipped; possible tiny inclusion
815093	-732	IMD	0.02	0.07	0.94	1.1	1.5	0.2	3.2	57.3	5.68	3.2	12.8	4.0	0.04	Euhedral
815125	-389	IMD	0.01	0.09	0.40	1.1	1.6	0.2	1.8	42.5	2.35	2.7	37.1	13.7	0.07	Euhedral
815144	-165	LDP	0.05	0.13	2.96	1.69	1.98	0.09	4.2	97.3	22.89	2.3	5.9	2.5	0.04	Broken in half
815096B	-795	IMD	0.02	0.05	0.74	1.4	1.8	0.2	3.1	55.3	6.32	2.6	8.2	3.2	0.03	Both ends chipped off
Rejected analyses																
815183[/4]	-22	DIO4	0.03	0.09	0.25	0.32	0.5	0.1	0.6	38.5	1.62	20.8	53.5	2.6	0.06	Very abraded; sample poor in general
815096[/5]	-795	IMD	0.01	0.02	0.28	5.16	7.5	0.6	3.0	40.5	2.53	3.0	6.6	2.2	0.13	Euhedral

Abbreviations. RL = elevation relative to mean sea level. Intrusions: DIO3 = intermineralization diorite porphyry 3 (Bayugo), DIO4 = late-mineralization diorite porphyry 4 (Bayugo), IMD = intermineralization diorite porphyry (Boyongan), LDP = late-mineral

[/1] Uncertainty (Unc.) reported at 2σ level.

[/2] Contribution of Sm to age determination.

[/3] Radius refers to the average of perpendicular half-widths of a tetragonal prism.

[/4] Young age suspect, given the small and abraded character of apatite crystal.

[/5] 7.5 Ma is geologically unreasonable, as it is older than U-Pb zircon ages for host intrusive suite (2.3 ± 0.1 to 2.1 ± 0.2 Ma).

APPENDIX DR4: RADIOCARBON GEOCHRONOLOGY

INTRODUCTION

Existing K-Ar and Ar-Ar age determinations for volcanic rocks from the Maniayao complex range between 600 and 90 ka. These rocks were collected from the surface from various parts of the complex prior to detailed drilling at Boyongan (Macpherson, 1999; Sajona et al., 1994; Sajona et al., 1997; UNDP, 1987). During subsequent drilling, intersection of intervals containing leaves and wood fragments (up to 70 cm in length) below the volcanics at the pre-Quaternary unconformity prompted a series of radiocarbon dates on this material to better constrain the onset of burial within the Mainit Graben in the vicinity of the Boyongan and Bayugo deposits.

METHODS

Samples of wood and of mud containing abundant plant material were collected from drilling intersections of the Tugunan Formation as close as possible to the basal unconformity. The three samples were dated at the Australian National University, and six at the Radiocarbon Dating Laboratory at the University of Waikato, New Zealand. The wood samples were leached with sodium chlorite to isolate the holocellulose fraction for dating. Sediment samples were disaggregated, washed, and a fraction of plant matter isolated for dating.

Six of the wood samples contained abundant material, and therefore were dated using conventional radiocarbon methods by conversion to benzene through hydrolysis of lithium carbide and catalytic trimerization of acetylene. The activity of ^{14}C of the benzene was measured using a Perkin Elmer 1220 Quantulus Liquid Scintillation spectrometer. The plant matter separates and the one holocellulose wood fraction were dated by accelerator mass spectrometry (AMS), owing to the paucity of sample material. Carbon in these samples was converted to CO_2 by catalysis with CuO at 800˚C, and then reduced to graphite with zinc at 600˚C using an iron catalyst. AMS age determinations were made on the graphite at the Rafter Radiocarbon Dating Laboratory at the Institute of Geological and Nuclear Sciences, New Zealand.

RESULTS

Of the nine samples dated, four contained essentially no detectable ^{14}C, and so are older than the detection limit for the method (41-45 ka). Age determinations for the remaining six samples were 30 and 1.6 ka (**Table DR6**).

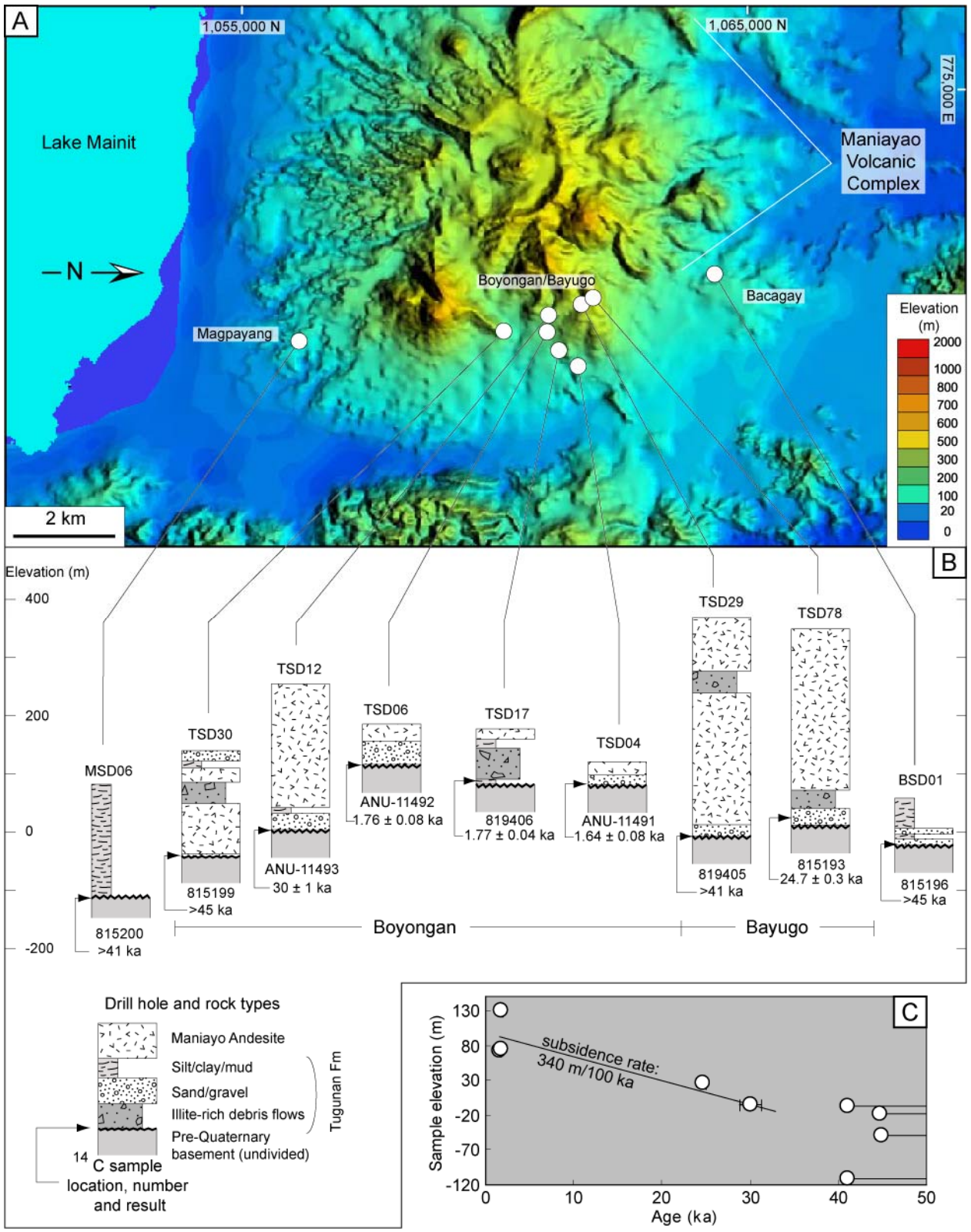

Figure DR7. Age constraints from the basal unconformity of the Tugunan Formation based on 14C dating of wood and other plant material. The surface digital elevation model (A) indicates the sample locations, while the stratigraphic sections generalized from drilling (B) emphasize the stratigraphic context and sampling elevation at the basal unconformity. The age determinations range between 30 and 1.6 ka, and display a consistent younging with sample elevation (C). Samples collected more than 8 m below sea level are older than the sensitivity range for 14C dating (~41 ka). Age determinations of less than 30 ka for samples overlying the Boyongan and Bayugo deposits attest to final burial in latest Pleistocene to Holocene time. These data suggest that the overlying Maniayao Andesite volcanic rocks in this area were deposited much more recently than indicated by available K-Ar age determinations for these rocks (600 - 90 ka). Digital elevation model modified after unpublished data from Anglo American Exploration (Philippines) Inc. Map Projection: UTM zone 51N, datum: Clark 1864 (Luzon exclusive of Palawan).

Table DR6. Radiocarbon dating of plant material near the base of the Tugunan Formation

Sample	Lab ID[/1]	Material Dated	Method[/3]	Result (ybp)[/4]	Unc. (ybp)[/5]	Description	Area	Borehole	Interval (m)	RL (m)[/6]	Position above contact (m)[/7]
	ANU-11491	Wood	RC	1640	80	Large (0.7 m) wood fragment from base of sandy gravel interval.	Boyongan	TSD04	40.4-41.1	73.5	1
	ANU-11492	Cellulose (wood)[/2]	RC	1760	80	Blackened wood fragments at base of a clay-rich gravelly sand sequence.	Boyongan	TSD06	52.75	130.3	3
819406	WK-19470	Cellulose (wood)	RC	1774	37	Sample from large (0.5 m) wood fragment (tree trunk?) in gravelly sand.	Boyongan	TSD17	105-105.15	75.0	1
815193	WK-19465	Cellulose (wood)	RC	24667	269	Wood fragment from sandy gravel interval.	Bayugo	TSD78	400.35-400.4	25.4	20
	ANU-11493	Leaves	RC	30,080	1270	Leaves and blackened wood fragments at base of a clay-rich gravelly sand sequence.	Boyongan	TSD12	290.82	-4.4	3
815200	WK-19468	Plant material	AMS	>41000		Massive silty clay with carbonaceous plant material and abundant fragments of a high-spire gastropod.	Magpayang	MSD06	183.22-183.32	-112.2	3
819405	WK-19469	Cellulose (wood)	AMS	>41000		Blackened fragments of wood collected from fissile sandy clay.	Boyongan	TSD29	327-327.1	-7.4	3
815199	WK-19467	Plant material	AMS	>45000		Massive silty clay with containing fragments of small bivalves, low-spire gastropods, and carbonaceous plant material.	Boyongan	TSD30	175.3-175.35	-49.3	2
815196	WK-19466	Cellulose (wood)	RC	>45000		Large wood fragment from gravelly clay interval.	Bagacay	BSD01	76.8-76.85	-17.8	15

[/1] Samples with numbers beginning with 'ANU' were dated at the Australian National University (ANU) by Chappell and Alimanovec (2003). All other samples dated at the University of Waikato by Hogg (2006).

[/2] Wood samples treated to concentrate the holocellulose fraction to provide the most robust age for old samples.

[/3] RC = conventional radiocarbon dating, AMS = accelerator mass spectrometry.

[/4] Years before present (1950), following the convention described by Stuiver and Polach (1977).

[/5] Uncertainty (Unc.) reported at 1σ level.

[/6] Elevation of the sample relative to modern mean sea level.

[/7] Sample position in meters above the unconformity atop the pre-Quaternary bedrock, as measured along the drill axis.

REFERENCES CITED

Braxton, D.P., 2007, Boyongan & Bayugo porphyry Cu-Au deposits, NE Mindanao, Philippines: geology, geochemistry, and tectonic evolution [PhD thesis]: Hobart, Australia, University of Tasmania.

Chappell, J., and Alimanovec, A., 2003, Report on Radiocarbon Age Determinations for ANU 11491-ANU 11493, Unpublished report prepared for Anglo American Philippines Inc.: Canberra, AUSTRALIA, Research School of Earth Sciences, Australian National University, p. 26.

Faure, G., 1986, Principles of Isotope Geology, John Wiley and Sons, 589 p.

Harrison, T.M., and Zeitler, P.K., 2005, Fundamentals of noble gas thermochronometry, *in* Reiners, P.W., and Ehlers, T.A., eds., Low-temperature thermochronology: Techniques, interpretations, and applications, Volume 58: Reviews in Mineralogy and Geochemistry, Mineralogical Society of America, p. 123-149.

Hogg, A., 2006, Report on radiocarbon age determinations for samples WK 19465-WK 19470: Hamilton, New Zealand, The University of Waikato Radiocarbon Dating Laboratory, p. 6.

Lee, J.K.W., Williams, I.S., and Ellis, D.J., 1997, Pb, U and Th diffusion in natural zircon: Nature, v. 390, p. 159-162.

Macpherson, C.G., 1999, Report on fieldwork in the Philippines; July-August 1999: London, United Kingdom, Southeast Asian Research Group, Royal Holloway, University of London, p. 65.

Markey, R., Hannah, J.L., Morgan, J.W., and Stein, H.J., 2003, A double spike for osmium analysis of highly radiogenic samples: Chemical Geology, v. 200, p. 395-406.

Merry, N., Pontual, S., and Gamson, P., 1999, The Spectral Geologist users manual v2.0, AusSpec International Pty Ltd., 146 p.

Paces, J.B., and Miller, J.D., Jr., 1993, Precise U-Pb ages of Duluth Complex and related mafic intrusions, northeastern Minnesota; geochronological insights to physical, petrogenetic, paleomagnetic, and tectonomagnetic processes associated with the 1.1 Ga Midcontinent Rift System: Journal of Geophysical Research, v. 98, p. 13,997-14,013.

Reiners, P.W., Spell, T.L., Nicolescu, S., and Zanetti, K.A., 2004, Zircon (U-Th)/He thermochronometry; He diffusion and comparisons with $^{40}Ar/^{39}Ar$ dating: Geochimica et Cosmochimica Acta, v. 68, p. 1857-1887.

Sajona, F.G., Bellon, H., Maury, R.C., Pubellier, M., Cotten, J., and Rangin, C., 1994, Magmatic response to abrupt changes in geodynamic settings; Pliocene-Quaternary calc-alkaline and Nb-enriched lavas from Mindanao (Philippines): Tectonophysics, v. 237, p. 47-72.

Sajona, F.G., Bellon, H., Maury, R.C., Pubellier, M., Quebral, R.D., Cotten, J., Bayon, F.E., Pagado, E., and Pamatian, P., 1997, Tertiary and Quaternary magmatism in Mindanao and Leyte (Philippines); geochronology, geochemistry and tectonic setting: Journal of Asian Earth Sciences, v. 15, p. 121-153.

Smoliar, M.I., Walker, R.J., and Morgan, J.W., 1996, Re-Os ages of Group IIA, IIIA, IVA, and IVB iron meteorites: Science, v. 271, p. 1099-1102.

Steiger, R.H., and Jager, E., 1977, Subcommission on geochronology: Convention on the use of decay constants in geo- and cosmochronology: Earth and Planetary Science Letters, v. 36, p. 359-362.

Stuiver, M., and Polach, H.A., 1977, Discussion; reporting of C-14 data: Radiocarbon, v. 19, p. 355-363.

Tera, F., and Wasserburg, G.J., 1972, U-Th-Pb systematics in three Apollo 14 basalts and the problem of initial Pb in lunar rocks: Earth and Planetary Science Letters, v. 14, p. 281-304.

UNDP, 1987, Geology and Gold Mineralization of Surigao del Norte, United Nations Development Programme: Manila, United Nations, p. 60.

Williams, I.S., 1998, U-Th-Pb geochronology by ion microprobe, *in* McKibben, M.A., Shanks, W.C.I., and W.I., R., eds., Applications of microanalytical techniques to understanding mineralising processes, Volume 7: Reviews in Economic Geology, p. 1-35.

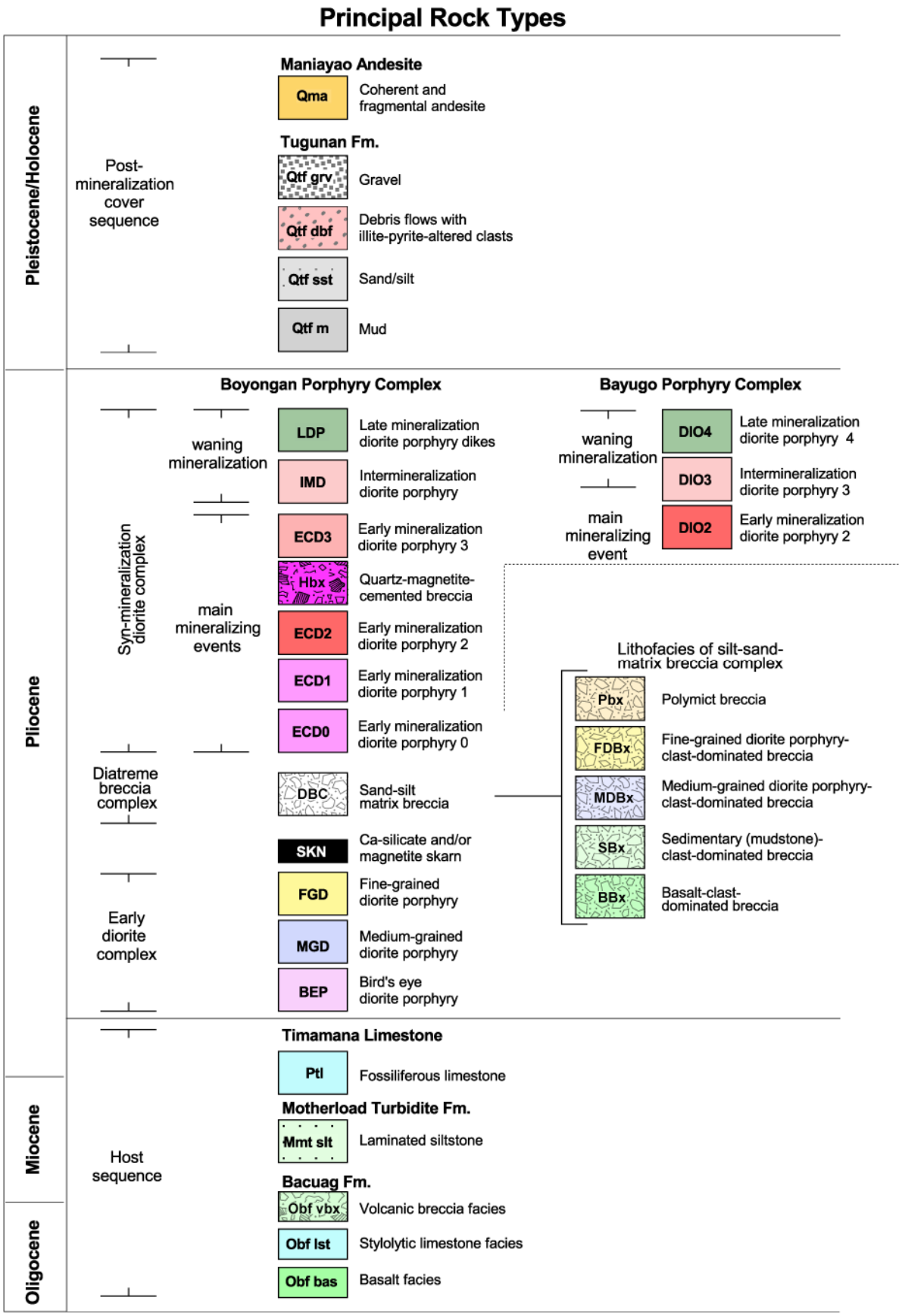

Legend Explanation of rock types depicted in maps and cross-sections (Figures DR1, DR5, and DR6).